European Polymer Journal 44 (2008) 2523–2528

Contents lists available at ScienceDirect

European Polymer Journal

journal homepage: www.elsevier.com/locate/europolj

Macromolecular Nanotechnology – Short communications

Pattern transfer fidelity in capillary force lithography with poly(ferrocenylsilane) plasma etch resists

Igor Korczagin, Hong Xu, Mark A. Hempenius, G. Julius Vancso *

MESA+ Institute for Nanotechnology, University of Twente, P.O. Box 217, 7500 AE Enschede, The Netherlands

ARTICLE INFO

Article history:
Received 31 March 2008
Received in revised form 19 May 2008
Accepted 23 May 2008
Available online 12 June 2008

Keywords:
Organometallic polymers
Pattern formation
Molecular parameters
Viscosity

ABSTRACT

The influence of processing conditions and polymer architecture on pattern transfer in capillary force lithography (CFL) using poly(ferrocenylsilane) etch resists is investigated. Zero-shear-rate viscosities measured at different temperatures and for polymers with different molar masses are related to the quality of CFL patterns, assessed based on atomic force microscopy experiments. An optimal range of viscosities corresponding to appropriate molar masses and processing temperatures is established. In this range, polymers possess enough mobility allowing for reasonably quick surface pattern formation. Yet, the polymers are not too mobile and preserve their shape when quenched to below T_g prior to serving as etch resist masks.

1. Introduction

Soft lithography can provide technically simpler and cheaper nano- and microfabrication alternatives to optical lithography, at least on a laboratory scale [1,2]. In order to successfully complement conventional photolithography, new functional materials must become available for soft lithography fabrication strategies. It has been shown that polymers and especially poly(ferrocenylsilanes) (PFS) [3] can be successfully employed as inks in soft lithographic applications. This organometallic polymer combines both macromolecular properties and a high etch resistivity in reactive plasmas. Because of the presence of iron and silicon atoms in the main chain, these polymers were found to be stable towards oxygen and fluorocarbon reactive ion etching [4]. This makes them ideal materials for "single step" resists. PFS was successfully employed in block copolymer lithography, where structures with smallest dimensions on the order of 20–30 nm were formed [5]. Thin films of PFS block copolymers could be used for direct pattern transfer of the microphase-separated morphology to underlying materials such as silicon [5], silicon nitride, or cobalt [6] to form dense arrays of nanoparticles on flat substrates. Block copolymer self-assembly on topographically patterned substrates produced long range ordered arrays of organometallic domains [7–10]. PFS was also used in soft lithography applications, such as micromolding in capillaries [4] and capillary force lithography [11].

In capillary force lithography (CFL) [12], capillarity forces the polymer melt into the void space of the channels formed between the mold and the polymer. The polymer confined initially in a thin film is squeezed out from the areas of contact between the PDMS mold and e.g. a Si substrate and develops microstructures along the vertical walls of the stamp. In other words the polymer is subjected to directed dewetting of the silicon substrate, guided by the stamp relief. The resulting patterns can be used as lithographic masks only when the polymer resist lines have a uniform thickness and no PFS remains on the silicon substrate between the lines. When the polymer film is kept in contact with the PDMS mold at too low a temperature or too briefly, polymer lines do not develop fully and PFS still remains between the lines. On the other hand, when the temperature is too high or the processing time too

* Corresponding author. Tel.: +31 53 489 2967; fax: +31 53 489 3823.
E-mail addresses: g.j.vancso@utwente.nl, epj@andoraconsulting.com (G. Julius Vancso).

0014-3057/$ - see front matter © 2008 Elsevier Ltd. All rights reserved.
doi:10.1016/j.eurpolymj.2008.05.034

long, dewetting of polymer patterns takes place. The outline of pattern development is schematically depicted in Fig. 1. Best polymeric lines are obtained at an optimal processing time and at a corresponding optimal temperature.

The dynamics of polymers in thin films determine in which regime patterning takes place. If the polymer is too mobile, the system is immediately in the dewetting regime. Conversely, a polymer with very slow dynamics does not reach the optimal pattern geometry. In order to get the desired patterns the lines have to be kinetically frozen by a combined control over structure dependent polymer viscosity and glass transition temperature (T_g). In order to estimate the optimal polymer mobility and corresponding processing temperature, we investigated the molar mass and temperature dependence of the polymer melt viscosity. This viscosity would then be related to the quality of polymer patterns, which was assessed based on AFM measurements. This allowed us to determine optimal viscosity limits for successful pattern transfer.

One has to bear in mind that the polymer under investigation is confined in an ultra-thin, 30 nm thick film. Attempts have been made to address mobility and viscosity of polymers confined in such thin films based on their dewetting kinetics [13]. Dewetting can be used as a probe of polymer mobility [14] and even to assess viscoelastic properties of the material [15]. However, in the case of CFL the situation is more complicated than in simple supported thin films. Capillary forces acting on polymer melts represent a driving force for directed dewetting of polymer confined in supported ultra-thin films. The resulting patterns are a product of the interplay between polymer mobility/viscosity and interfacial tensions. Rather than looking into the mobility of polymer in thin films, we decided to simply measure bulk values of the zero-shear-rate viscosity and relate these to the quality of CFL patterns. This approach is based on the assumption that polymer viscosity in thin films is related to molar mass and temperature in the same manner as in the bulk.

In summary, this work provides an investigation of structure–property relationships of PFS polymers used as inks in soft lithography (CFL). By varying molar mass, the viscosity of the polymer can be tuned, allowing an optimal processing temperature to be used in the patterning process.

2. Experimental section

2.1. Materials

Ferrocene, *N,N,N′,N′*-tetramethylethylenediamine (TMEDA), dichlorosilanes (dimethyl- and ethylmethyl), and *n*-butyllithium were purchased from Aldrich. The corresponding [1]silaferrocenophanes were prepared as described earlier [16–19]. Polydimethylsiloxane (PDMS) molds were prepared with Sylgard 184 silicone elastomer (Dow Corning). Prepolymer was mixed with curing agent in a 10:1 ratio. The mixture was degassed under vacuum, poured onto a pre-patterned silicon master and cured at 100 °C.

2.2. Polymerisations

A mixture of [1]ethylmethylsilaferrocenophane (13 wt%) and [1]dimethylsilaferrocenophane (87 wt%) was dissolved in THF in a glovebox purged with prepurified nitrogen. The polymerization was initiated by the addition of *n*-butyllithium (0.16 M in hexanes) [17,20]. The living polymerization was carried out at 20 °C and terminated after 30 min by adding a few drops of degassed methanol. The

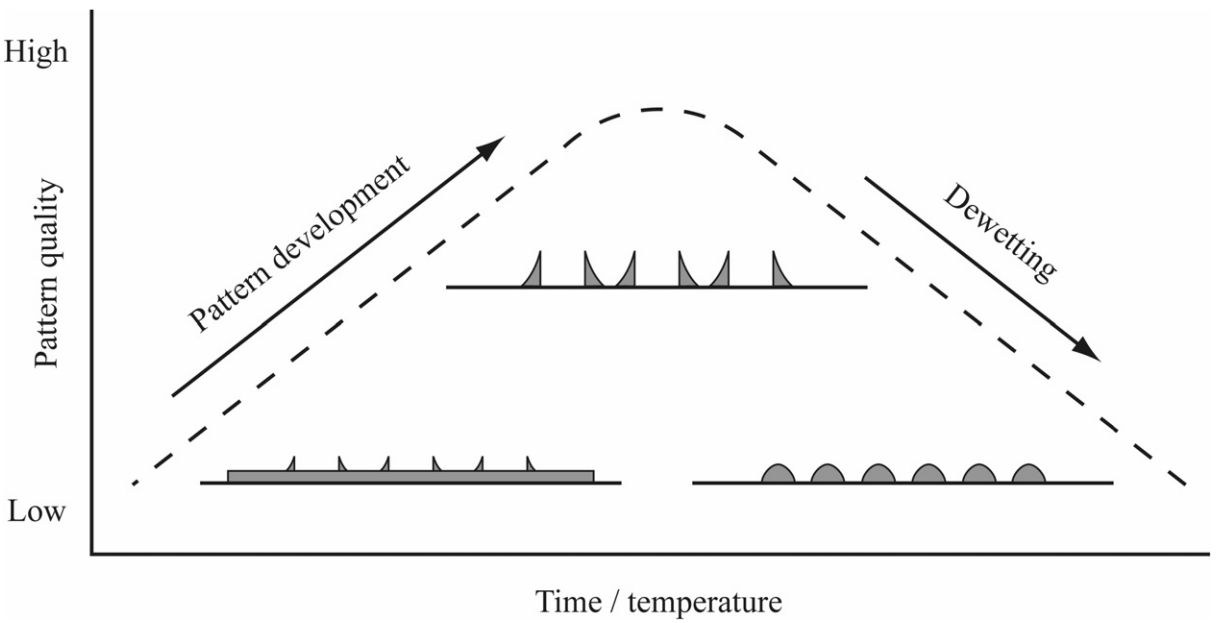

Fig. 1. Schematic presentation of pattern quality development in capillary force lithography/directed dewetting.

polymer was precipitated in methanol and dried under vacuum.

2.3. Instrumentation

GPC measurements were carried out in THF at 25 °C, using microstyragel columns (bead size 10 mm) with pore sizes of 10^5, 10^4, 10^3 and 10^6 Å (Waters) and a dual detection system consisting of a differential refractometer (Waters model 410) and a differential viscometer (Viscotek model H502). Molar masses were determined relative to polystyrene standards. A Perkin–Elmer Pyris 1 Differential Scanning Calorimeter was used for the determination of glass transition temperatures (T_g) and isothermal crystallization experiments. Temperature scans were performed from −35 °C to 160 °C at a scan rate of 10 K/min. Isothermal crystallizations were carried out by quenching the samples from the melt to 70 °C. Silicon substrates were cleaned in a microwave oxygen plasma reactor Tepla 300E (500 W, 0.5 Torr O_2, 5 min). Polymer films were spin-coated onto silicon wafers or PDMS stamps from toluene solutions. Film thicknesses were determined with a Plasmos SD 2002 ellipsometer, using a wavelength of 632.8 nm. A Digital Instruments NanoScope IIIa atomic force microscope (Veeco, Digital Instruments) was used to obtain images of the surface morphology of the samples. Standard Si_3N_4 tips were used (Pointprobe, Nanosensors) with an average tip radius of 10 nm. Images were acquired in ambient air using the tapping mode. The amplitude of oscillation at free vibration was A_0 = 1.5 V with operating setpoint ratios A/A_0 = 0.6–0.9, scan size was 50 μm and scan rate 0.301 Hz. Viscosity measurements were performed on a Physica UDS 200 rheometer using a parallel plate configuration. The gap between the plates was 0.5 mm and a shear strain of 1% was applied. Dynamic viscosities were measured at frequencies from 0.01 to 50 Hz as a function of temperature between 30 °C and 150 °C with steps of 10 °C. Zero-shear-rate viscosities were calculated by extrapolation of the viscosity values using an exponential function model for each isothermal scan. Mastercurves were constructed from the isothermal frequency sweeps and shifted to a reference temperature of 80 °C using the principle of time-temperature superposition (WLF equation).

2.4. Pattern formation

The polymer micro-patterns were fabricated by placing the PDMS mold in contact with the thin polymer films (20 nm) and keeping it there for 4 h at temperatures ranging from 30 to 140 °C, in vacuum. The stamp was removed at room temperature and resulting polymer microstructures were imaged by atomic force microscopy.

3. Results and discussion

3.1. Choice of materials

The ideal polymeric materials for CFL should have a T_g above room temperature in order to preserve the shape of the formed microstructures after stamp removal. Crystalline polymers are not suitable for CFL fabrication because annealing of polymer samples takes place at temperatures as close to T_g as possible to retain the resulting pattern. Crystallization may under such conditions lead to pattern destruction. Finally, polymers used in CFL should have an appropriate etch resistivity in order to faithfully replicate patterns into underlying substrates. PFSs can fulfil all of the above requirements. Thermal properties of PFSs can be tuned by choosing proper substituents at the Si atom. Symmetrically substituted poly(ferrocenylsilanes) are not suited for CFL because of their semicrystalline nature. Unsymmetrically substituted, amorphous poly(ferrocenylsilanes) constitute a better choice for CFL patterning. Indeed, poly(ferrocenylmethylphenylsilane) was successfully employed in CFL experiments [11]. However, attempts to synthesize high molar mass, unsymmetrically substituted PFSs via anionic polymerization failed. To examine a range of polymers with different molar masses and to assess their utility in CFL pattern transfer, statistical copolymers of [1]ethylmethylsilaferrocenophane (13 wt%) and [1]dimethylsilaferrocenophane (87 wt%) were prepared. Unsymmetrically substituted ferrocenylsilane units incorporated in poly(ferrocenyldimethylsilane) suppress crystallization of this polymer [20]. In this way an amorphous PFS with a T_g above room temperature was obtained.

Table 1
Molecular and thermal characteristics of PFS statistical copolymers obtained from [1]ethylmethylsilaferrocenophane (13 wt%) and [1]dimethylsilaferrocenophane (87 wt%)

Polymer	M_n (g/mol)[a]	M_w/M_n	T_g (°C)[b]
1	3.100	1.10	35.0
2	6.500	1.04	36.8
3	15.700	1.04	38.5
4	65.700	1.08	38.8

[a] Measured by GPC in THF, relative to polystyrene standards.
[b] Glass transition temperatures (T_g) were obtained at a scan rate of 10 K/min.

Isothermal crystallization experiments performed by DSC showed no crystallization exotherms. No melting peaks were observed upon heating. This indicates that the added unsymmetrically substituted monomer prevents the crystallization of poly(ferrocenyldimethylsilane). Polymers with different molar masses were synthesized. The dependence of the T_g on the molar mass was investigated. It was fitted with O'Driscoll's equation [21] and the extrapolated value of T_g of the polymer with infinite molar mass was found to be 39.6 °C. The molecular and thermal characteristics of the polymers are given in Table 1.

3.2. Viscosity measurements

Oscillatory shear flow experiments were performed on a rheometer in a parallel plate configuration. The polymer samples were sinusoidally sheared according to $\gamma(t) = \gamma_0 \sin\omega t$ and $\dot{\gamma}(t) = \omega\gamma_0 \cos\omega t$ where γ_0 is the amplitude of sinusoidal deformation, $\dot{\gamma}$ is the shear rate and ω the angular frequency. For linear viscoelastic behavior a sinusoidally varying strain is associated with a sinusoidally varying stress $\sigma = \gamma_0(G' \sin\omega t + G'' \cos\omega t)$ where G' and G'' are

the frequency dependent shear storage and shear loss moduli. It is convenient to express the sinusoidally varying stress as a complex quantity. Then the modulus is also complex, given by $\sigma^*/\gamma_0 = G^* = G' + iG''$ and $G''/G' = \tan\delta$, where δ is the phase angle between stress and strain, and $\tan\delta$ is the damping factor. The dissipative effects of alternating stress can be described by the ratio of stress in phase with strain rate and the strain rate. This has the dimensions of viscosity and is the real part η' of the complex viscosity, $\eta^* = \eta' - i\eta''$ defined in the same manner as G^* [22]. In sinusoidal deformations $\eta^* = G^*/i\omega$, and the individual components are related by $\eta' = G''/\omega$ and $\eta'' = G'/\omega$. At very low frequencies, the in-phase or real component η' approaches η_0, the zero-shear viscosity. It is clear from the above equations, that in regions where G'' is flat, the dynamic viscosity is inversely proportional to frequency and when G'' rises steeply, on the left side of a maximum, the viscosity can flatten out (Fig. 2). The dynamic rheological measurements offer much more information than just polymer viscosity. By employing this technique one can observe time, frequency and temperature influences on mechanical properties of polymers. In an amorphous polymer above its glass transition temperature, a single empirical function can describe the temperature dependence of all mechanical and electrical relaxation processes. The ratio (α_T) of any mechanical relaxation time at temperature T to its value at a reference temperature, T_0 (e.g. $\alpha_T = \frac{\eta(T)}{\eta(T_0)}$) derived from transient or dynamic viscoelastic measurements appears to be identical over wide ranges of time scale [23].

An example of a mastercurve of polymer **3** constructed using the above principle is shown in Fig. 2. Measurements were carried out at temperatures varying from 50 to 120 °C and subsequently shifted to the reference temperature of 80 °C using the time-temperature superposition principle. At low frequencies the slopes of 2 and 1 are clearly visible, which is in agreement with theoretical predictions (Maxwell model) [22,24].

The shear viscosity η is one of the principle quantities determining the rheological behavior of polymer melts. In our experiments frequency sweeps were performed on each of the PFS polymers (Table 1) at different temperatures. At every measurement point the viscosity was calculated as a ratio of shear stress and shear rate. At sufficiently low shear rates the viscosity approaches a limiting constant value η_0, the zero-shear-rate viscosity, which is not measured directly, but found by extrapolation of viscosity values as a function of shear rate. Models that describe the relationship between shear rate and viscosity for non-Newtonian liquids include the exponential Ostwald–de Waele model, Bird-Carreau model and many others [25]. Our measurement data were fitted with the following simple exponential function:

$$\eta = \eta_0 \exp(-A\dot{\gamma})$$

where A is a constant. This model provided an excellent fit to the experimental data especially at higher temperature. The magnitude of η_0 depends on temperature, molar mass and hydrostatic pressure [26]. Polymer viscosity decreases with increasing temperature due to an increase in polymer chain mobility and free volume between the chains. The temperature dependence of shear viscosity can be described by the following exponential equation:

$$\eta_0 = A \exp\left(\frac{B}{T - T_0}\right)$$

where A is a constant, B corresponds to the activation temperature and T_0 is the Vogel temperature. This equation is often referred to as the Vogel–Fulcher law and is equivalent to the more general Wiliams, Landel and Ferry equation (WLF) [22,23].

For each of the PFS polymers (presented in Table 1), η_0 was measured as a function of temperature between 30 and 150 °C. An example of viscosity values obtained for polymer **3** is shown in Fig. 3. All polymers exhibited typical pseudoplastic, shear thinning behavior. Increasing the temperature resulted in a decrease in the zero-shear-rate viscosity values. It is interesting to observe how the flow properties of polymer **3** cross over from non-Newtonian at lower temperatures (50–90 °C) to Newtonian at temper-

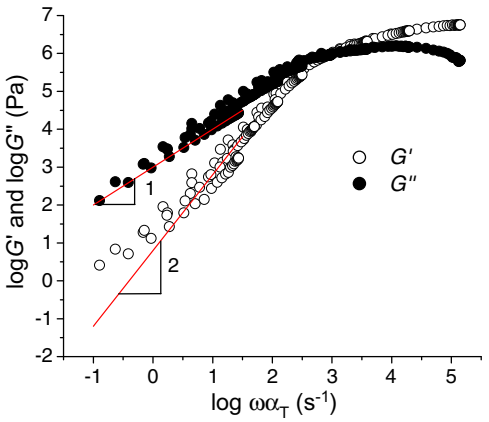

Fig. 2. Double logarithmic plot of the dynamic moduli (G' and G'') of polymer **3** vs. reduced angular frequency ($\omega\alpha_T$). Measurements were carried out at temperatures varying from 50 to 120 °C. The reference temperature was set at 80 °C.

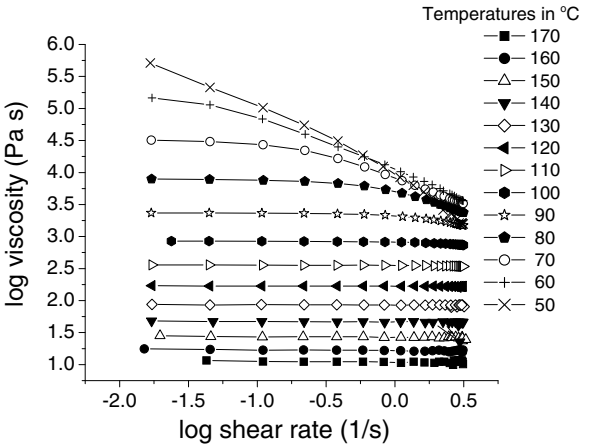

Fig. 3. Viscosity of polymer **3** measured at low shear rates and at different temperatures.

atures above 90 °C. A similar transition was also observed for polymers **1** (between 40 and 50 °C) and **2** (between 50 and 60 °C). Conversely, polymer **4** demonstrated non-Newtonian behavior within the experimental temperature and shear rate ranges. This is the first indication of the influence of molar mass on the flow properties of PFS polymers, reflected later in the quality of surface patterns. Subsequently, the viscosity values were related to the quality of corresponding polymer patterns obtained by CFL.

3.3. Capillary force lithography

The patterns in capillary force lithography experiments were fabricated by placing the PDMS mold in contact with the 20 nm thin polymer films and keeping it for 4 h at temperatures ranging from 30 to 140 °C, under vacuum. The PDMS stamp geometry used consisted of 5 μm wide recessed lines spaced by 3 μm wide protruding lines (denoted as 3 × 5 μm). The polymer, initially confined in a thin film, is squeezed out from areas of contact between the stamp and silicon substrate. It diffuses into the grooves where structures are formed along the vertical walls of the stamp due to capillary rise. Very thin polymer films do not provide enough material to fill the grooves of the stamp completely [27]. As a result, two polymeric lines are formed per one groove. This is clearly seen in section analyses of the AFM images (Fig. 4).

Fig. 4 shows an example of polymer patterns obtained at 100 °C. Two top images show low molar mass polymers **1** and **2** (3.1 and 6.5 kg/mol) with corresponding viscosities

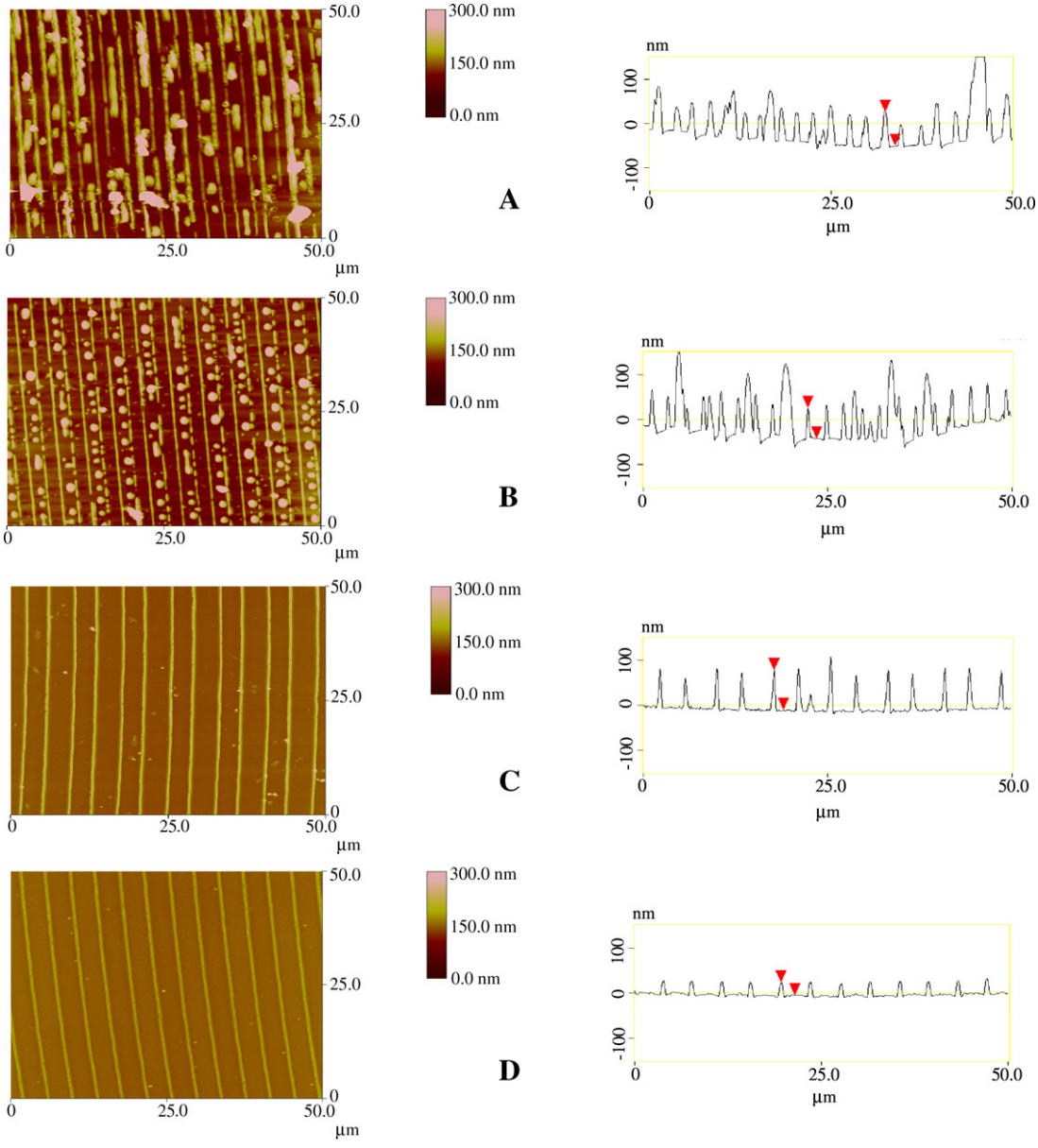

Fig. 4. AFM height images and section analysis of polymer patterns prepared by CFL (4 h at 100 °C). From top to bottom: polymers **1**, **2**, **3** and **4**, respectively.

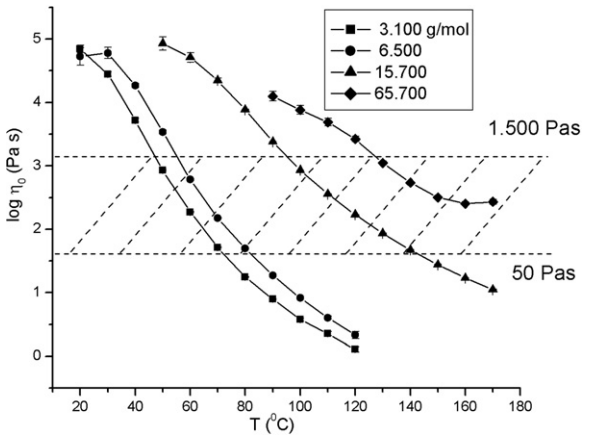

Fig. 5. Molar mass/temperature dependence of zero-shear-rate viscosity of PFS. The marked region shows optimal viscosities for successful pattern transfer in capillary force lithography.

of 3.8 and 8.2 Pa s, respectively. Patterns obtained with these materials show coalescence of polymer into droplets as a result of polymer dewetting. Fig. 4C demonstrates patterns obtained under the same processing conditions, using polymer **3** with a molar mass of 15.7 kg/mol (η_0 = 850 Pa s). The polymer lines are well developed with a height on the order of 100 nm. Finally, CFL of polymer **4** with the highest molar mass (65.7 kg/mol, η_0 = 7600 Pa s) at 100 °C resulted in incompletely developed lines with a height of 30 nm, with the polymer remaining between the lines. A similar analysis of pattern quality was performed for all the polymers in the temperature range of 30–140 °C.

From the analysis of AFM measurements, a proper temperature range for pattern transfer by CFL for polymers with different molar masses is obtained. Combination of these results with the rheological data yields the optimal range of viscosities for a successful pattern transfer in CFL. Most of the good quality patterns were prepared with polymers of which viscosities fall into the range between 50 and 1500 Pa s (Fig. 5). When these findings are related to the viscosity profiles as shown in Fig. 3, it becomes evident that best surface patterns were obtained with polymers in the Newtonian (viscous) flow regime.

4. Conclusions

There are three main parameters that have a direct impact on the quality of CFL polymer patterns: molar mass of a polymer, processing temperature (and time) and initial polymer film thickness. We found that the right balance between T_g and processing conditions (viscosity) is essential for successful patterning. On the one hand polymers with too low a viscosity will easier dewet, and on the other hand polymers with too high a viscosity will not yield patterns within the experimental time scale. Thus, the zero-shear-rate viscosity of a polymer melt is a very important factor that will influence the quality of the patterns. A range of optimal viscosities for pattern formation was established. This information was used to optimize conditions for CFL pattern transfer. Viscosity values obtained from bulk rheological measurements were related to the quality of polymer micropatterns, assessed based on AFM analysis. We are aware of the fact that dynamics at polymer surfaces and in thin films can differ substantially from the bulk, nevertheless our results present a clear trend and could prove very useful for any micro(nano)fabrication strategy involving capillary force lithography, especially since these results have a more universal character and can be applied to other polymers.

Acknowledgements

The authors gratefully acknowledge the University of Twente and the Masif Program of the MESA$^+$ Institute for Nanotechnology for financial support. HX acknowledges Delta National scholarship for financial support.

References

[1] Xia YN, Whitesides GM. Angew Chem Int Ed 1998;37:551.
[2] Odom TW, Love JC, Wolfe DB, Paul KE, Whitesides GM. Langmuir 2002;18:5314.
[3] (a) Manners I. Chem Commun 1999:857;
(b) Kulbaba K, Manners I. Macromol Rapid Commun 2001;22:711;
(c) Whittell GR. Adv Mater 2007;19:3439.
[4] Lammertink RGH, Hempenius MA, Chan VZH, Thomas EL, Vancso GJ. Chem Mater 2001;13:429.
[5] Lammertink RGH, Hempenius MA, van den Enk JE, Chan VZH, Thomas EL, Vancso GJ. Adv Mater 2000;12:98.
[6] Cheng JY, Ross CA, Chan VZH, Thomas EL, Lammertink RGH, Vancso GJ. Adv Mater 2001;13:1174.
[7] Cheng JY, Ross CA, Thomas EL, Smith HI, Vancso GJ. Appl Phys Lett 2002;81:3657.
[8] (a) Cheng JY, Ross CA, Thomas EL, Smith HI, Vancso GJ. Adv Mater 2003;15:1599;
(b) Cheng JY, Zhang F, Smith HI, Vancso GJ, Ross CA. Adv Mater 2006;18:597.
[9] Cheng JY, Mayes AM, Ross CA. Nat Mater 2004;3:823.
[10] Roerdink M, Hempenius MA, Gunst U, Arlinghaus HF, Vancso GJ. Small 2007;3:1415.
[11] Korczagin I, Golze S, Hempenius MA, Vancso GJ. Chem Mater 2003;15:3663.
[12] Suh KY, Kim YS, Lee HH. Adv Mater 2001;13:1386.
[13] Masson JL, Green PF. Phys Rev E 2002;65:031806.
[14] Reiter G. Macromolecules 1994;27:3046.
[15] Seemann R, Herminghaus S, Jacobs K. Phys Rev Lett 2001;87:196101.
[16] Fisher AB, Kinney JB, Staley RH, Wrighton MS. J Am Chem Soc 1979;101:6501.
[17] Ni Y, Rulkens R, Manners I. J Am Chem Soc 1996;118:4102.
[18] Temple K, Massey JA, Chen Z, Vaidya N, Berenbaum A, Foster MD, Manners I. J Inorg Organomet Polym 1999;9:189.
[19] Lammertink RGH, Hempenius MA, Thomas EL, Vancso GJ. J Polym Sci, Part B 1999;37:1009.
[20] Roerdink M, Hempenius MA, Vancso GJ. Chem Mater 2005;17:1275.
[21] O'Driscoll K, Sanayei RA. Macromolecules 1991;24:4479.
[22] Ferry JD. Viscoelastic properties of polymers. New York: John Wiley & Sons; 1970.
[23] Williams ML, Landel RF, Ferry JD. J Am Chem Soc 1955;77:3701.
[24] Tschoegl NW. The phenomenological theory of linear viscoelastic behavior. An introduction. Berlin, Heidelberg, New York: Springer; 1989.
[25] (a) Bird RB, Armstrong RC, Hassager O. Dynamics of polymeric liquids. 2nd ed. New York: Wiley; 1987;
(b) Bird RB, Stewart WE, Lightfoot EN. Transport phenomena. 2nd ed. New York: John Wiley & Sons Inc.; 2002.
[26] van Krevelen DW. Properties of polymers: their correlation with chemical structure; their numerical estimation and prediction from additive group contributions. Amsterdam: Elsevier; 1990.
[27] Suh KY, Yoo PJ, Lee HH. Macromolecules 2002;35:4414.